Journal of
Ceramic Science
and Technology

J. Ceram. Sci. Tech., **03** [04] 159-168 (2012)
DOI: 10.4416/JCST2012-00025
available online at: http://www.ceramic-science.com

Mechanical Characterization of PZT Ceramics for Multilayer Piezoelectric Actuators

R. Bermejo*[1], M. Deluca[1, 2]

[1]Institut für Struktur- und Funktionskeramik (ISFK), Montanuniversitaet Leoben, Peter-Tunner Strasse 5, A-8700 Leoben, Austria
[2]Materials Center Leoben Forschung GmbH, Roseggerstrasse 12, A-8700 Leoben, Austria
received July 22, 2012; received in revised form August 01, 2012; accepted August 28, 2012

Abstract

Multilayer piezoelectric actuators (MPA) are commonly used to control injection valves in modern combustion engines operating in a temperature range from -40 °C up to 125 °C. They consist of a stack of very thin piezoceramic layers, mostly based on Lead Zirconate Titanate (PZT) material with interdigitated metallic electrodes in between. In this work the mechanical properties of both pure piezoceramic material and the multilayer structure are investigated in terms of strength and crack growth resistance. The results of strength tests are interpreted in the mainframe of Weibull theory, and fractographic analyses are performed in order to get information about the weakest links in the microstructure. The crack growth resistance is determined using the single-edge V-notched beam (SEVNB) method in both materials to estimate the influence of the electrodes on crack propagation. The influence of the texture (i.e. domain-orientation) is assessed with indentation techniques under combined mechanical and thermal loads. In addition, with the aid of Raman spectroscopy it is shown that crack growth anisotropy is intimately linked with domain switching segregation; cracks arrest earlier when propagating along a direction where domain switching is highly favored. Based on experimental results, guidelines for an improved design of MPA are also given.

Keywords: Piezoelectric multilayer actuator, domain switching, strength, fracture resistance, Raman spectroscopy

I. Introduction

The outstanding piezoelectric properties of piezoceramics are widely employed in the fabrication of sensors and actuators used in applications that require precision displacement control or high generative forces, i.e. precision mechanoelectronic and semiconductor devices. The demanding requirements for advanced devices have involved in many cases the combination of material classes (such as metals, ceramics and polymers) to fulfill the performance in a given system. In these cases, the fabrication of components having two different materials has been a challenge, not only from the viewpoint of the structural integrity (i.e. mechanical resistance) of the part but also from its functionality. For instance, modern multilayer piezoelectric actuators (MPA) used in advanced injection systems consist of a stack of thin piezoceramic layers which are separated by very finely printed metallic electrodes (see Fig. 1). The integration of electrodes into ceramic parts requires a precise location of the interdigitated structure as well as high piezoelectric properties of the piezoceramic to fulfill the performance in service [1, 2]. Owing to this design, high electric fields and large elongations can be reached with relatively low voltages [3]. The main feature of the actuator's functionality is associated with the domain switching process triggered by an electrical field (ferroelectricity) and/or mechanical loading (ferroelasticity).

* Corresponding author: raul.bermejo@unileoben.ac.at

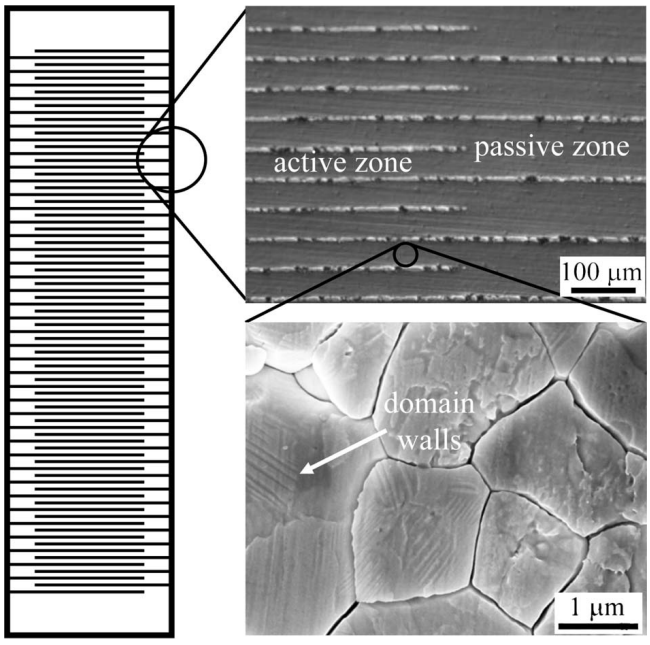

Fig. 1: Multilayer piezoelectric actuator scheme used in fuel injection systems. A detail of the active and passive zones is presented.

The most common material employed as piezoceramic is Lead Zirconate Titanate ($PbZr_{1-x}Ti_xO_3$, PZT) in the neighborhood of the Morphotropic Phase Boundary (MPB) (i.e. x = ~0.48) owing to the high strain response

that is caused by enhanced domain switching capability – an extrinsic effect [4–7]. The corresponding strains are of the order of 0.1 % (for a typical stack length of about 40 mm the elongation is approximately 40 μm). This elongation can be attained in a very short time (in the order of milliseconds), allowing for fast and accurate fuel flow into the combustion chamber. The effectiveness of such an injection process (low fuel consumption, reduction of emissions) is based on the reliable functionality of the MPA over its lifetime, i.e. order of 10^9 cycles. In this regard, the relatively large displacements and large forces within the MPA along with the combined thermal, electrical and mechanical loadings yield nonlinear effects, which may lead to degradation of the performance of the MPA [8, 9]. In service, for instance, the actuating-process is indeed a result of the periodic reorientation (domain switching) of the piezoelectric crystals in the PZT in the ferroelectric phase, i.e. below the Curie temperature. During this process, cyclic inelastic deformation and Joule heating occur. These effects may lead to periodic tensile stresses concentrated around the electrode tips [10], which can induce fatigue damage (the growth of cracks) in the ceramic material, thus affecting the structural and functional integrity of the MPA. In addition, although these MPA operate under externally applied compressive stresses, failure of components in service has been reported associated with the propagation of cracks within the electrode-ceramic multilayered structure [10]. The functionality of such devices is associated with the mechanical resistance of the ceramic layers; if cracks propagate between electrodes, the device cannot fulfill its function anymore [11, 12]. Therefore, to ensure such high reliability of the ceramic components, uncontrolled propagation of cracks must be avoided completely. The investigation of the initiation and subsequent growth of cracks in piezoceramic materials is of primary importance and has been the focus of many researchers. Considerable work has been done to analyze the behavior of monolithic piezoceramics to determine the strength and crack growth resistance with respect to defined electrical boundary conditions [8, 13–22].

In the present work, the mechanical behavior of commercial PZT material used in MPA devices is illustrated in terms of strength and fracture toughness (resistance to crack propagation). Four-point bending tests are performed on both bulk ceramic samples and multilayer metal-ceramic composites to investigate the influence of electrodes and domain texture on the flexural strength distribution. The results of strength tests are interpreted in the mainframe of Weibull theory. Fractographic analyses are performed in order to retrieve information about the type and location of the defect causing the failure. The fracture toughness of the piezoceramic material (with and without electrodes) is measured using the Single-Edge V-Notch Beam (SEVNB) method to evaluate the effect of the electrodes on crack propagation. Furthermore, the influence of texture (i.e. domain-orientation) is assessed using indentation techniques on poled specimens, exploring the effect of temperature and mechanical load on the possible depolarization of the material. These studies are substantiated by the analysis of domain texture in the material with polarized Raman spectroscopy, thus allowing a direct connection between crack growth resistance and domain switching.

II. Statistical Nature of Mechanical Strength in PZT

The strength of brittle materials, σ_f, can be determined with standardized four-point bending (4PB) tests. According to Griffith's analysis [23], the strength scales with the fracture toughness, K_{Ic}, and is inversely proportional to the square root of the critical crack size a_c:

$$\sigma_f = \frac{K_{Ic}}{Y\sqrt{\pi a_c}} \quad (1)$$

Y is a geometric correction factor which may also depend on the loading situation [24–26]. For cracks that are small compared to the component size (this is generally the case in ceramics), Y is of the order of unity.

Strength test results on ceramic specimens show, in general, large scatter. This follows from the fact that in each individual specimen the size and location of the critical defect (or crack) can be different. Typical volume flaws, which may act as fracture origins, are second phase regions, large pores, inclusions, large grains or agglomerations of small pores [27]. Common fracture origins at the surface are grinding scratches and contact damage. Even grooves at grain boundaries may act as fracture origins. Another consequence of the strength scatter is associated with the toughness of the material. In case the material presents an increasing resistance to crack propagation with the crack length (the so-called R-curve), K_{Ic} may depend on the crack length. The stress measured at fracture (according to Eq. 1) can thus differ from specimen to specimen depending on the loading level and on the size of the critical defect. It has been shown that PZT possesses a pronounced R-curve due to domain switching acting at the crack tip [8, 15, 17, 18, 20, 22]. The resistance to crack propagation does not only depend on the polarization state of the PZT but also on the direction in which the crack advances. This is known as toughness anisotropy in PZT.

The interpretation of strength results in PZT ceramics can be done in the framework of Weibull statistics, assuming that an homogeneous crack-size frequency density function $g(a)$ exists. In most materials the size frequency density of the cracks decreases with increasing crack size. i.e. $g \propto a^{-p}$, with p being a material constant [28, 29]. This lets us derive the well-known relationship for Weibull statistics [30, 31]:

$$F(\sigma,V) = 1 - \exp\left[-\frac{V}{V_0}\left(\frac{\sigma}{\sigma_0}\right)^m\right] \quad (2)$$

The Weibull modulus m describes the scatter of the strength data. The characteristic strength σ_0 is the stress at which, for specimens of volume $V = V_0$, the failure probability is $F(\sigma_0, V_0)=1-\exp^{(-1)} \approx 63\%$. Note that the modulus m is related to the size distribution of the cracks, i.e. $m = 2(p-1)$. For more details see [28, 32].

III. Experimental Methods

(1) Determination of flexural strength

In order to illustrate the effect of domains on the strength distribution in PZT, standard 4PB tests (spans: 30 – 15 mm)

have been performed on (i) non-poled bulk PZT ceramic specimens, (ii) non-poled and poled multilayer metal-ceramic composites, to assess the influence of the microstructure on the strength of the material [33]. The multilayer composite consists of several PZT layers interdigitated with metal electrodes. Dimensions of the specimens were 35 mm x 3.0 mm x 2.25 mm (length x width x height), the electrodes having an area of 35 mm x 3.0 mm and a thickness of ca. 5 μm. A total of 30 specimens were tested for each sample using a universal testing machine (Zwick Z010, Zwick/Roell, Ulm, Germany) with a 200 N load cell. Flexural tests were performed under displacement control at ambient conditions (T = 25 °C and 25 % RH), using a relatively high displacement rate of 1.5 mm/min to avoid environmental effects [34]. The equivalent "elastically" bending stress, σ_e, was calculated following the EN-843 – 1 standards [35]:

$$\sigma_e = \frac{3F(S_0 - S_i)}{2bh^2} \quad (3)$$

where F (in N) is the fracture load, S_o and S_i are the outer and inner spans (30 mm and 15 mm), respectively, b (in mm) is the specimen width and h (in mm) is the specimen height.

(2) Fractographic analysis

Optical examination of fracture surfaces was performed with an Olympus BX50 light microscope, an Olympus SZH10 stereo microscope (Olympus, Tokyo, Japan), and with a Quanta 200 Mk2 FEG-SEM (FEI, Hillsboro, OR, USA) scanning electron microscope.

(3) Evaluation of fracture toughness

The resistance to crack propagation is a very important property to describe the mechanical behavior of brittle materials. The propagation of a crack normal to the applied stress field leads to the Mode I fracture, which is in most cases the common failure mode of a ceramic. The fracture toughness, K_{Ic}, is the material property related to such mode of fracture. It can be measured using the Single-Edge V-Notch Beam method (SEVNB), which constitutes the only standard method for fracture toughness measurements in brittle materials [36]. According to this procedure, K_{Ic} can be determined on a notched specimen of length a in a 4PB test following the norm standards EN-843 – 1 [35]. The fracture toughness can be evaluated according to [36]:

$$K_{Ic} = \sigma_f \cdot Y \cdot \sqrt{a} \quad (4)$$

where σ_f is the failure stress (in MPa), a is the crack length (in m) and Y is a geometric factor defined for an edge crack and given as [36]:

$$Y(\delta) = 1.9887 - 1.326\delta - \left[\frac{(3.49 - 0.68\delta + 1.35\delta^2) \cdot \delta(1 - \delta)}{(1 + \delta)^2}\right] \quad (5)$$

and

$$\delta = a/W \quad (6)$$

where W (in m) is the specimen thickness.

The mode I fracture toughness in PZT has been determined in bulk specimens. To account for the effect of the electrodes on the resistance to crack propagation, SEVNB tests have also been performed on non-poled multilayer structures similar to those used for strength measurements. The notched specimens can be seen in Fig. 2.

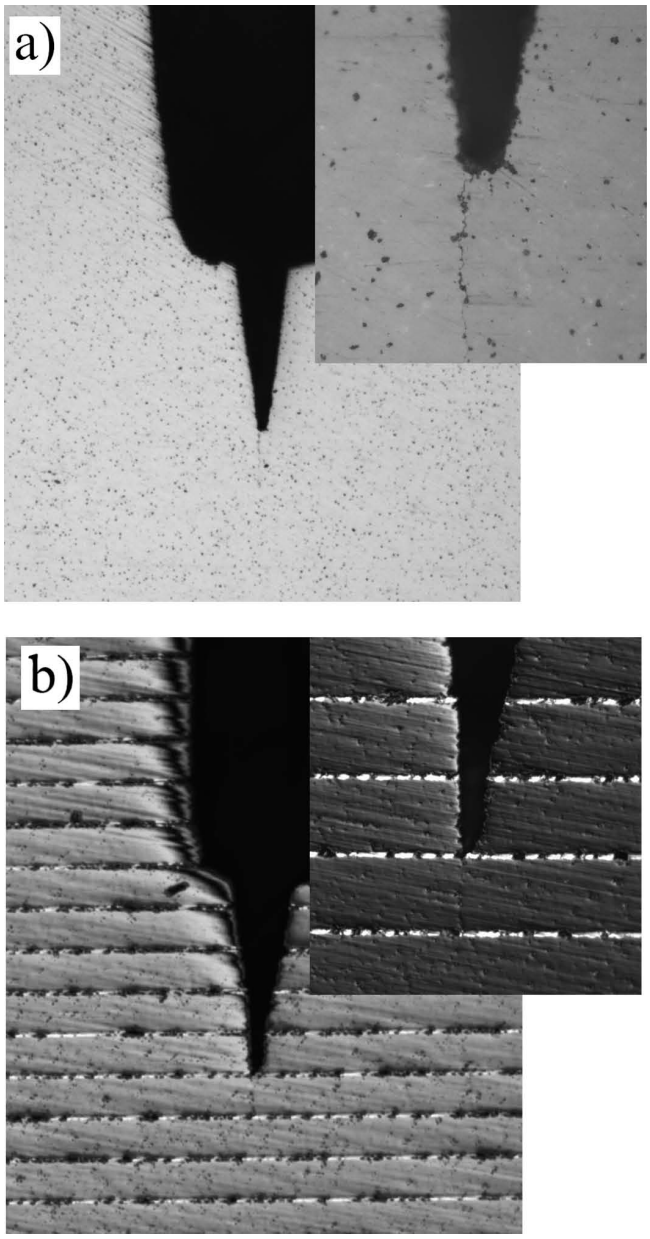

Fig. 2: a) Bulk and b) multilayer PZT notched specimens for fracture toughness determination using the SEVNB method.

(4) Crack growth resistance: effect of domain switching

In order to investigate the effect of domain orientation on the fracture resistance of the material, the indentation fracture (IF) method was employed. At least five indentations with 1 kg load were placed along the polished surface of each specimen in a way that the resulting cracks were parallel or perpendicular to the direction of the applied electrical field (i.e. specimen longitudinal direction). The crack growth resistance (CGR) can be evaluated following the relation proposed by Anstis *et al.* [37], namely by measuring the length of the indentation cracks both parallel ($2c^{//}$) and normal ($2c^{\perp}$) to the longitudinal axis of the specimen:

$$K_R = \chi \cdot \frac{P}{c^{3/2}} \quad (7)$$

Here χ is a parameter related to the shape of the indentation crack, P (in N) is the indentation load and c (in m) is half the length of the measured indentation crack. The χ parameter has been estimated based on the K_{Ic} value calculated above with the SEVNB method on an "as-sintered" PZT (i.e. non-poled) material [38].

(5) Crack growth resistance: effect of temperature and mechanical load

The service conditions under which MPA operates involve mechanical loading and rapid temperature changes (effective temperature range: -40 °C to 125 °C, considering heating from ambient to combustion temperature during winter months). In order to simulate, to some extent, the real thermo-mechanical fracture behavior of the PZT ceramic material during service, the crack growth resistance of a doped PZT ceramic is investigated using the indentation method explained above. Combined thermal and mechanical loads are first applied to poled (bulk) specimens with dimensions (10 mm x 4 mm x 3 mm) by means of a temperature chamber (Carbolite GmbH, Ubstadt-Weiher, Germany) coupled to an adapted universal testing machine (Messphysik Materials Testing GmbH, Fürstenfeld, Austria). The compressive stress, applied along the poling direction (i.e. largest dimension of the specimen), forces the domains to switch perpendicularly with respect to the stress (poling) axis (ferroelastic effect). After the tests, the specimens are removed from the testing set-up and indentation cracks are introduced in the tested specimens at room temperature. The crack lengths of the indentations are measured (parallel and normal to the poling direction) and compared with the initial indentations cracks on poled specimens. Using Eq. (7), the crack growth resistance in both directions is determined.

IV. Results and Discussion

(1) Flexural strength and failure analyses

Fig. 3a shows the strength distribution versus the probability of failure of the three different samples, represented in a Weibull diagram. Owing to the non-linear behavior of PZT during bending, the true outer fiber stress, σ^*, was estimated from the elastically calculated bending stress, σ_e, according to Fett *et al.* [39]. According to this, the true outer fiber stress is a function of the level of elastically stress associated with the elastic strain during bending. For the case of non-poled specimens σ^* may be around 70 % of σ_e, while for the poled samples σ^* may read only approx. 60 % of σ_e (for details see [39]).

In Fig. 3b the (outer fiber) characteristic strength, $\sigma_0{}^*$, is plotted versus the Weibull modulus, m, for each sample. The 90 % confidence intervals, defined as the range which contains the true parameters (i.e. $\sigma_0{}^*$ and m) with a probability of 90 %, are also represented in the referred figure by vertical and horizontal bars respectively. It can be observed that both $\sigma_0{}^*$, and m are not affected by the presence of electrodes (compare poled and non-poled samples). However, a clear difference between poled and non-poled multilayer materials is observed (Fig. 3b): the poling state of the material does affect its strength distribution (represented by the Weibull modulus, m). In Table 1 the Weibull parameters with the 90 % confidence intervals are listed for the three samples.

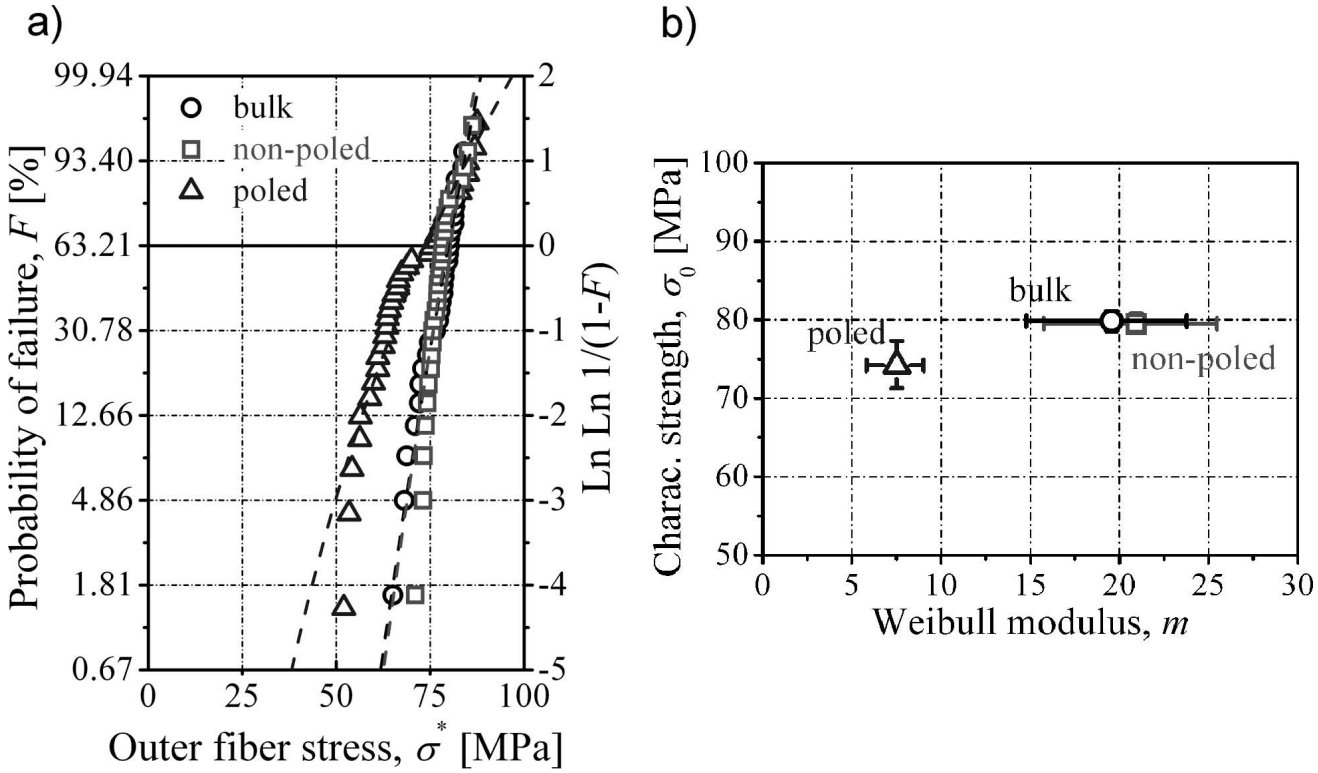

Fig. 3: a) Strength distribution vs. probability of failure in a Weibull diagram, and b) characteristic strength vs. Weibull modulus of (i) non-poled bulk ceramic specimens, (ii) non-poled and (iii) poled multilayer metal-ceramic composites.

Table 1: Elastically calculated and outer fibre characteristic strength, s_0 and σ_0^*, and Weibull modulus, m, for non-poled bulk and multilayer samples as well as for poled multilayer specimens. The 90 % confidence intervals are also listed.

Sample	Characteristic Strength [MPa]		Weibull modulus, [–]
	σ_0	σ_0^*	m
Bulk (non-poled)	114 (112 – 116)	80 (79 – 81)	20 (15 – 24)
Multilayer (non-poled)	113 (112 – 115)	80 (78 – 81)	21 (16 – 26)
Multilayer (poled)	124 (119 – 129)	74 (71 – 77)	8 (6 – 9)

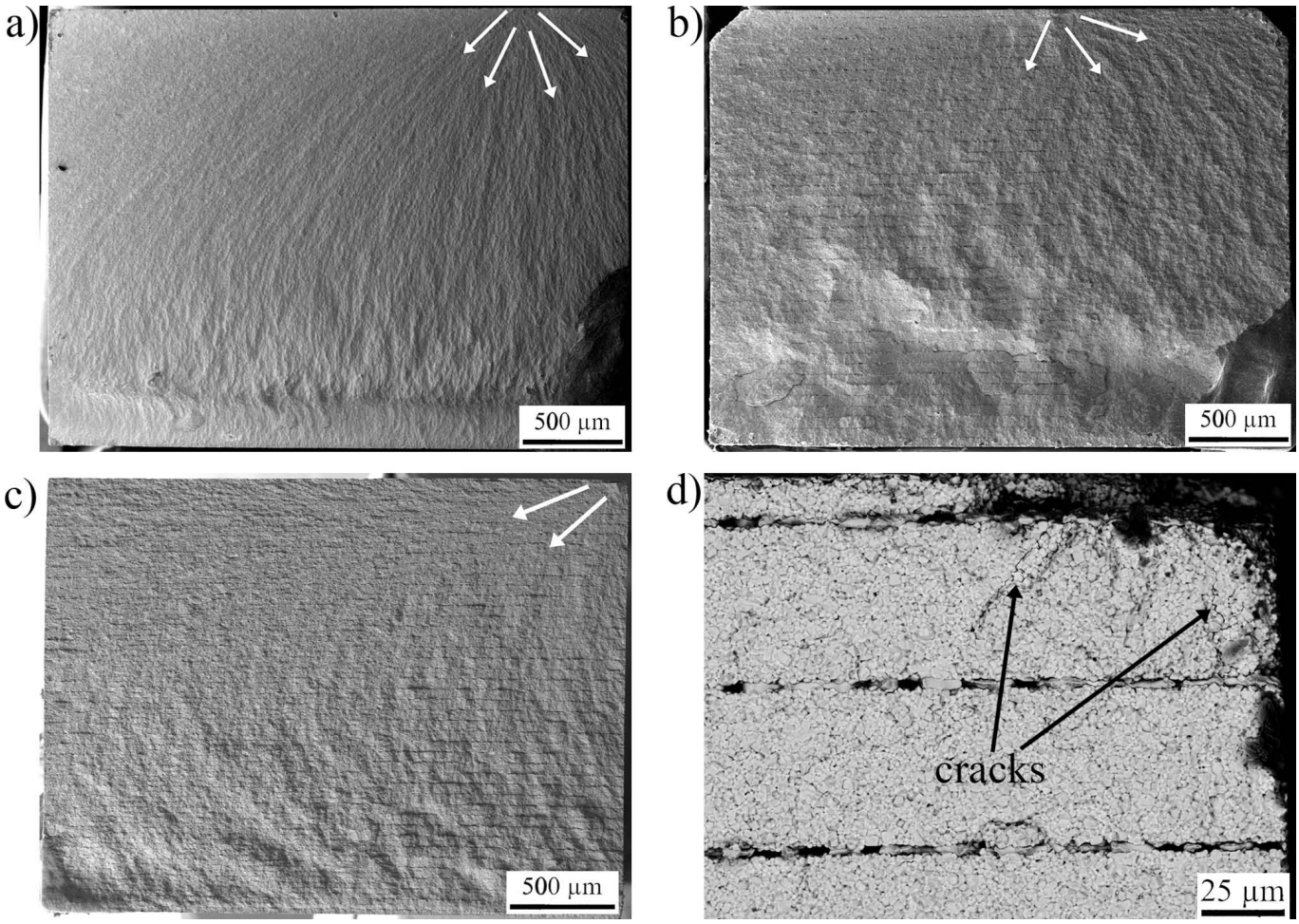

Fig. 4: SEM micrographs of the fracture surfaces of a) non-poled PZT bulk monolith, b) non-poled and c) poled multilayer metal-PZT-ceramic composite. The fracture is intergranular and initiates at the tensile surface (arrows indicate fracture propagation). In d) some cracks can be observed in the poled multilayer metal-PZT-ceramic composite, which originated during poling.

A fractographic analysis of broken specimens is shown in Fig. 4 with reference to the three different samples. The fracture origin for (i) bulk and (ii) non-poled specimens is likely to be found at the surface tested under tension (see Figs. 4a and 4b). On the other hand, in the poled multilayers (iii) the fracture originates in some cases at the edges of the specimen (see Fig. 4c). Crack propagation is indicated by the direction of hackle lines (evidenced by white arrows in Figs. 4a, 4b and 4c). In other cases microcracks could be found at the fracture surfaces (see Fig. 4d) which have originated during the poling operation. As a result, the lower Weibull modulus in the poled specimens can be ascribed to the coexistence of both inherent natural flaws and relatively large cracks. In terms of strength this cannot be clearly appreciated in Fig. 3a owing to the small size of the sample tested. However, microcracks could be found at the fracture surface of specimens with lower strength.

(2) Fracture toughness: influence of metal electrodes

The toughness values calculated according to Eq. (4) are $K_{Ic,b} = 1.1 \pm 0.1$ MPa·m$^{1/2}$ and $K_{Ic,m} = 1.5 \pm 0.1$ MPa·m$^{1/2}$ for bulk and multilayer respectively. The positive effect of the metal electrodes on the crack growth resistance is associated with their plastic deformation. It can be inferred that a crack propagating in a bulk PZT will require less applied stress than propagating through a metal-ceramic multilay-

er architecture. The query arises whether the direction of propagation in multilayer devices (i.e. parallel or perpendicular to the electrodes) may be different, influenced by the crack growth resistance of the PZT material in different directions (i.e. toughness anisotropy). This phenomenon can be investigated using indentation techniques to induce cracks in poled and non-poled PZT material [11, 15], and will be explored in the next section.

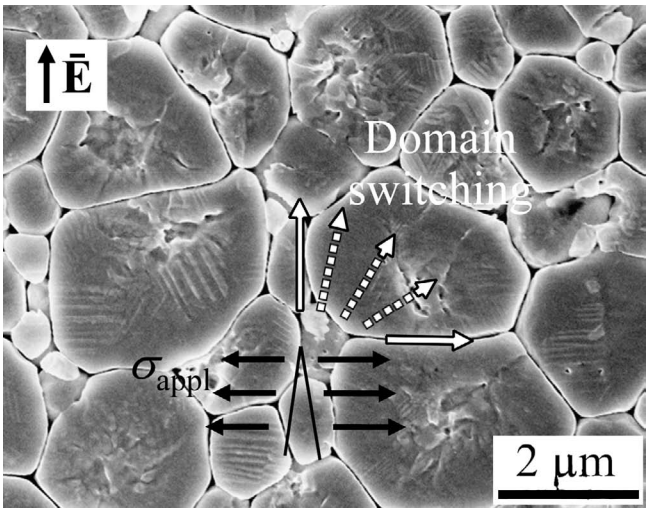

Fig. 5: Schematic of domain switching process in front of a crack tip.

(3) Crack growth resistance

(a) *Effect of domain switching*

A crack in a material can grow when the applied stress intensity factor, K_I, overcomes the toughness of the material K_{Ic}. In an isotropic material, the resistance to crack propagation results in the same in all directions. This is also the case in non-poled PZT, where domains are randomly oriented and thus the microstructure can be considered as homogeneous. However, in a poled PZT a significant amount of domains are oriented along the axis where the electrical field (**E**) has been applied (poling axis). Now the microstructure is no longer uniform and a preferential direction for crack propagation exists. When a crack propagates parallel to the poling direction under the application of an external mechanical stress field, tensile stresses exist at the crack tip (see Fig. 5). In a poled PZT material, domains located around the crack tip may switch owing to the ferroelastic effect (Fig. 5). This switching process consumes energy which is then no longer available to advance the crack [38]. As a result, the crack growth resistance (CGR) is higher along the poling direction. This phenomenon is illustrated in Fig. 6 with indentation cracks. For non-poled materials, in which domains are randomly oriented in all directions, crack lengths are the same in both parallel and perpendicular directions (i.e. the CGR is identical in all directions), as expected for an isotropic material. On the other hand, in poled specimens the CGR is influenced by the preferred orientation of domains. Here cracks in direction of poling are smaller than in the perpendicular direction owing to ferroelastic domain switching. The CGR has been evaluated using Eq. (7). The χ parameter has been estimated as 0.11 ± 0.01 based on the K_{Ic} value for non-poled PZT calculated with SEVNB (i.e. $K_{Ic,b} = 1.1 \pm 0.1\ \mathrm{MPa \cdot m^{1/2}}$). For an applied indentation load of 1 kg, the fracture resistance values parallel and normal to the poling axis resulted in $K_R^{//} = 1.51 \pm 0.02\ \mathrm{MPa \cdot m^{1/2}}$ and $K_R^{\perp} = 0.62 \pm 0.01\ \mathrm{MPa \cdot m^{1/2}}$ respectively.

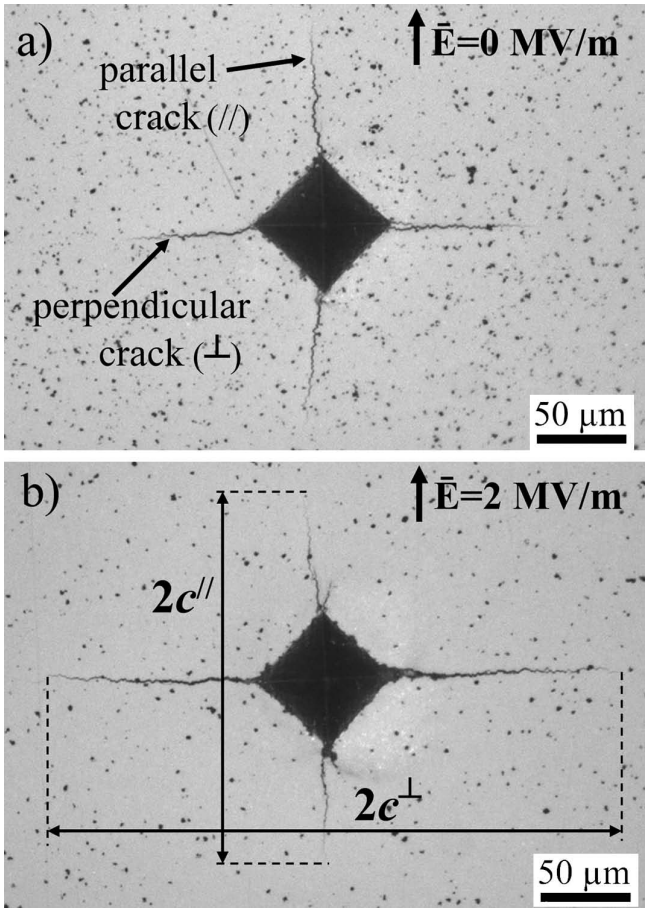

Fig. 6: Indentation cracks parallel and perpendicular to the longitudinal direction in a) non-poled specimens, i.e. **E** = 0 MV/m, and b) poled specimens, i.e. **E** = 2 MV/m.

(b) *Depolarization effects*

In Fig. 7a a light effect of temperature (i.e. depolarization) can be appreciated on the poled specimens up to the Curie temperature, whereas for the non-poled sample no temperature effects are observed. In Fig. 7b the combined effect of temperature and mechanical load (i.e. 50 MPa in compression) is shown. In this case a significant depolarization effect was observed after lower exposure temperatures. Interesting are the tests at temperatures of approx. 225 °C, where the fracture resistance in both parallel and normal directions result in the same, i.e. $K_R^{//} = 1.04 \pm 0.02\ \mathrm{MPa \cdot m^{1/2}}$ and $K_R^{\perp} = 1.04 \pm 0.01\ \mathrm{MPa \cdot m^{1/2}}$ respectively. These values coincide with the ones reported for the non-poled specimens (Fig. 7a). Although the CGR of the material may not be isotropic at this temperature, there are two different domain orientation distributions yielding the same CGR in the directions parallel and normal to the poling axis. Above this temperature (i.e. > 225 °C) and owing to the relatively high applied compressive stress (σ = -50 MPa), the fracture resistance anisotropy reverses, yielding higher crack growth resistance in the direction normal to the longitudinal axis

(Fig. 7b). This phenomenon can be already observed below the Curie temperature, even for lower compression loads (see details in [38]). Finally, for temperatures beyond the Curie point (e.g. 400 °C), the fracture resistance normal to the longitudinal direction can reach values up to $K_R^{\perp} = 1.75\ MPa{\cdot}m^{1/2}$, that is, even higher than $K_R^{//}$ at room temperature (corresponding to a hypothetical electrically "fully" poled PZT material). However, the increase in fracture resistance normal to the longitudinal axis is counterbalanced by a decrease in the parallel direction. In other words, the shielding effect associated with the increase amount of domains oriented in the normal direction (in case of MPA parallel to the electrodes) will yield a corresponding decrease of the fracture resistance in the other direction, i.e. perpendicular to the electrodes. This effect may be of importance in the case of multilayered actuators, where the propagation of cracks from outer terminal electrode through the whole stack to the other outer electrode (i.e. parallel to the poling direction) may cause the failure of the actuator.

V. Design Guidelines to Improve Fracture Resistance of PZT in Multilayer Actuators

Crack propagation in structural and functional ceramics has been investigated by many authors in recent decades in order to understand the fracture process in ceramic materials. Particular attention has been paid to multilayered structures where the properties of the individual layers could be tailored to influence the fracture behavior of the layered material. In this regard, layered structures designed with weak interfaces, crack growth resistance (R-curve) behavior through microstructure design and/or residual stresses among others, have shown outstanding potential for structural applications, showing enhanced fracture toughness by means of energy dissipating mechanisms such as interface delamination and/or crack deflection/bifurcation phenomena. A review can be found in [40]. The understanding of the conditions under which such mechanisms occur and the influence of the layered architecture (e.g. geometry, composition of layers, elastic and physical properties of the layers) on the crack propagation is the key feature to obtain tougher and more resistant and reliable materials and components. The architecture of multilayered actuators (stacks), where the ceramic layers are stacked between electrode sheets, resembles the design of layered structural ceramics. Within this context, a similar approach used in layered ceramics to control crack propagation could be attempted in MPA. The complex stress distribution during the fabrication of MPA and the later poling process to meet the service requirements can lead to the generation of cracks that may affect the structural and functional integrity of the stack. In this regard, two strategies may be adopted in order to improve the performance of these components: 1) avoid the formation of cracks within the stack optimizing both the processing and poling process, and 2) assuming that cracks are distributed within the component, try to control the crack propagation so that the functionality of the stack is not affected. The complexity increases owing to the interaction of the electrical charges and the mechanical loads of different kind in the metal-ceramics layered materials.

A major problem that may be encountered in this type of layered designs is the deflection of propagating cracks from one electrode towards the other, leading to short-circuit of the component, and thus failure of its functionality. A crack connecting two electrodes of opposite polarity would constitute a free channel with very low dielectric permittivity (the permittivity of air is much lower than that of the ceramic), thus increasing the chance of disruptive discharge.

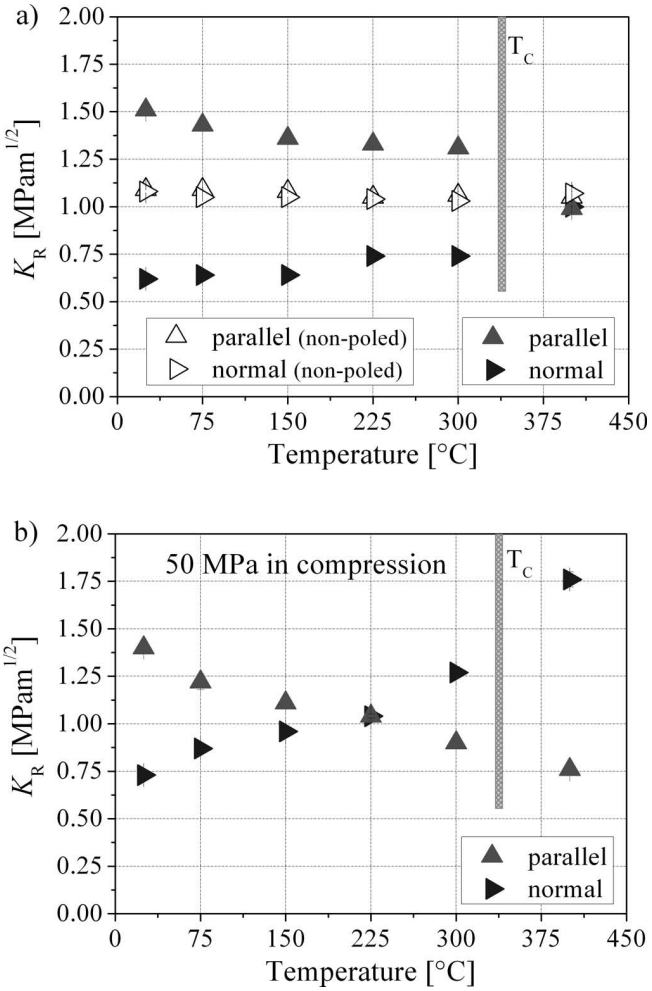

Fig. 7: Crack growth resistance measured in poled PZT specimens after exposure at a) different temperatures and b) combining temperature and mechanical load (i.e. 50 MPa in compression). Non-poled specimens are also shown in a) for comparison. A slight effect of the temperature on K_R can be appreciated on the poled specimens, leading to partial depolarization. This is more acute when mechanical compressive load is also applied parallel to the poling direction.

Therefore, an immediate query is raised whether the path that the propagating crack follows, i.e. along or near the electrode (where the crack initiates), may be influenced by the design parameters, such as geometry and/or mechanical properties of the different piezoceramic layers, to avoid crack propagation between electrodes, so that the component can increase its lifetime durability. In this regard, the benefits of high failure resistance materials designed with weak interfaces and the mechanical reliability enhancement (flaw tolerance) of residual-stress-based materials designed with strong interfaces could be combined in a unique multilayer architecture, as has been reported

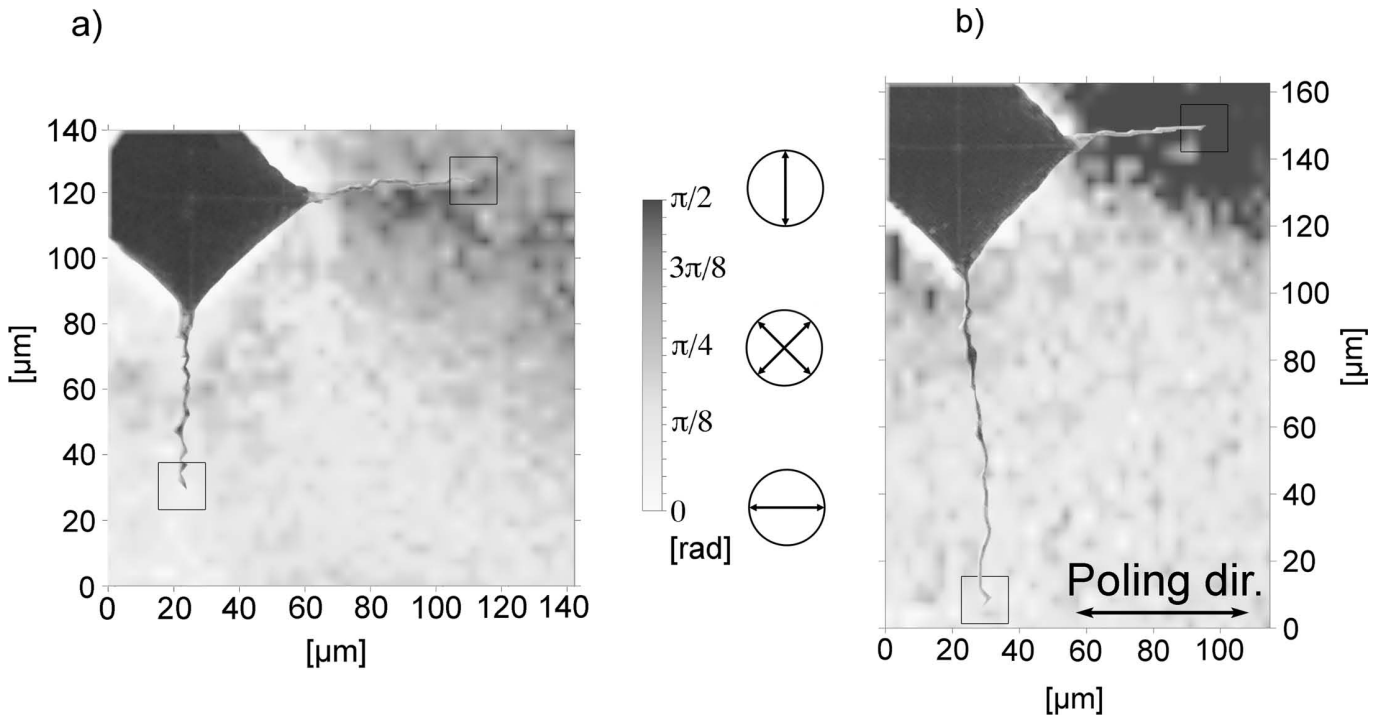

Fig. 8: Domain orientation in both a) non-poled and b) poled PZT bulks by means of polarized Raman spectroscopy. Sampling was performed with 4-µm steps. The domain orientation is reported as an angle with respect to the incident laser polarization, maintained always horizontal (i.e. coincident with the poling direction in b). (Reproduced from [46]).

elsewhere [41]. For instance, weak interfaces in piezo-actuators could act as locations which would favor crack propagation, thus avoiding the propagation of cracks between electrodes (short circuit). In addition, the introduction of "protective" layers with residual stresses (e.g. a compressive layer to stop the propagation of subcritical propagating cracks [42]) in the design could increase its lifetime and reliability.

In addition to this, new experimental methods are needed to investigate the *in-situ* domain switching responsible for CGR anisotropy in PZT-based materials. Also thermo-mechanical strains in certain regions of multilayer devices can lead to degradation and failure of the actuator. A promising approach is the utilization of polarized Raman spectroscopy for strain analysis. This technique is well known in the field of materials science for being an easy-to-use non-destructive technique with micrometer-scale spatial resolution. The use of polarized incident light at the same time as analyzing the scattered light polarization allows information to be obtained on the local orientation of the crystal structure. Details on this technique can be found in the literature, applied on various semiconductor and ceramic materials (see for instance [43, 44]). In piezoelectric ceramics, the intensity of Raman modes is strongly dependent on the local orientation of ferroelectric domains. If it is assumed that the texture is unchanged in the investigated area, polarized Raman spectra can be used to perform microscale mapping of local orientations in areas of interest, such as in the neighborhood of Vickers indents [45, 46]. As an example, Fig. 8 shows Raman domain mapping in the vicinity of indentations that were placed on both non-poled (Fig. 8a) and poled (Fig. 8b) PZT bulks at room temperature, without any prior conditioning of the sample. As expected, the non-poled material presents cracks growing with the same length in each direction, whereas the poled sample presents cracks that are shorter parallel to the poling direction and longer perpendicularly, compared to the non-poled case. This is reflected in a higher amount of domain switching in the vicinity of the parallel crack, whereas on the perpendicular crack little or no domain switching occurred. In the non-poled sample, both cracks present the same amount of domain switching. The relationship between CGR (calculated with the IF method described above) and domain switching (calculated considering the measured orientation and the orientation far away from the indentation in both samples) has been reported elsewhere [46]. It demonstrates that higher domain switching produces high CGR, and vice-versa, with respect to the non-poled case. Crack growth anisotropy is thus intimately linked with domain switching segregation: cracks arrest earlier when propagating along a direction where domain switching is highly favored. On the other hand, in directions where no domain switching occurs, the measured K_R value can be regarded as the CGR of the PZT material in the absence of any toughening mechanism.

VI. Conclusions

The mechanical properties of Lead Zirconate Titanate (PZT) material used in Multilayer Piezoelectric Actuators (MPA) have been investigated in terms of strength and crack growth resistance. The distribution function of strengths determined from experimental bending tests is dependent on the poling state of the material and on its structure, and is conditioned by the presence of cracks generated during the poling process. The crack growth resistance (CGR) can be influenced by the texture (i.e. domain-orientation), which may be enhanced under com-

bined mechanical and thermal loads. The use of Raman spectroscopy in the vicinity of cracks showed that CGR anisotropy is intimately linked with domain switching segregation; cracks arrest earlier when propagating along a direction where domain switching is highly favored. Recommendations to increase the fracture resistance in MPA are given based on layered designs.

References

1 Uchino, K.: Piezoelectric actuators and ultrasonic motors. In Electronic Materials: Science and technology. H.L. Tuller, Kluwer Academic Publishers, (1997).

2 Setter, N.: Piezoelectric materials in devices: Ceramics laboratory, EPFL, Swiss Federal Institute of Technology, (2002).

3 Pritchard, J., Bowen, C.R., Lowrie, F.: In multilayer actuators: Review, Vol. 100. British Ceramic Transactions, (2001).

4 Noheda, B., Gonzalo, J.A., Cross, L.E., Guo, R., Park, S.-E., Cox, D.E., Shirane, G.: Tetragonal-to-monoclinic phase transition in a ferroelectric Perovskite: the structure of $PbZr_{0.52}Ti_{0.48}O_3$, *Phys. Rev. B,* **61**, 8687 – 8695, (2000).

5 Frantti, J., Ivanov, S., Eriksson, S., Rundlöf, H., Lantto, V., Lappalainen, J., Kakihana, M.: Phase transitions of $Pb(Zr_xTi_{1-x})O_3$ ceramics, *Phys. Rev. B,* **66**, 064108, (2002).

6 Woodward, D.I., Knudsen, J., Reaney, I.M.: Review of crystal and domain structures in the $PbZr_xTi_{1-x}O_3$ solid solution, *Phys. Rev. B,* **72**, 104110, (2005).

7 Helke, G., Lubitz, K.: Piezoelectric pzt ceramics. In Piezoelectricity: Evolution and future of a technology edited by W. Heywang, K. Lubitz and W. Wersing, Berlin, 89 – 131, (2009).

8 Cao, H., Evans, A.G.: Non-linear deformation of ferroelectric ceramics, *J. Am. Ceram. Soc.,* **76**, 890 – 896, (1993).

9 Supancic, P., Wang, Z., Harrer, W., Reichmann, K., Danzer, D.: Strength and fractography of piezoceramic multilayer stacks, *Key Engng. Mat.,* **290**, 46 – 53, (2005).

10 Furata, A., Uchino, K.: Dynamic observation of crack propagation in piezoelectric multilayer actuators, *J. Am. Ceram. Soc.,* **76**, 1615 – 1617, (1993).

11 Lynch, C.: Fracture of ferroelectric and relaxor ceramics: influence of electric field, *Acta Mater.,* **46**, 599 – 608, (1998).

12 Kuna, M.: Fracture mechanics of piezoelectric materials – where are we right Now?, *Eng. Fract. Mech.,* **77**, 309 – 326, (2010).

13 Wang, H., Wereszczak, A.A.: Effects of electric field on the biaxial strength of poled PZT. In: Advances in electronic ceramics: Ceramic engineering and science proceedings, **28**, (8), John Wiley & Sons, Inc., 57 – 68 (2009).

14 Calderon-Moreno, J.M., Guiu, F., Meredith, M., Reece, M.J.: Fracture toughness anisotropy of PZT, *Mat. Sci. & Eng.,* **A234 – 236**, 1062 – 1066, (1997).

15 Schneider, G.A., Heyer, V.: Influence of the electric field on vickers indentation crack growth in $BaTiO_3$, *J. Eur. Ceram. Soc.,* **19**, 1299 – 1306, (1998).

16 Schneider, G.A., Heyer, V.: Influence of the electric field on vickers indentation crack growth in $BaTiO_3$, *J. Eur. Ceram. Soc.,* **19**, 1299 – 1306, (1999).

17 Kolleck, A., Schneider, G.A., Meschke, F.: R-curve behaviour of $BaTiO_3$ and PZT ceramics under the influence of an electric field applied parallel to the crack front, *Acta Mater.,* **48**, 4099 – 4113, (2000).

18 Meschke, F., Raddatz, O., Kolleck, A., Schneider, G.A.: R-curve behavior and crack-closure stresses in barium titanate and (Mg,Y)-PSZ ceramics, *J. Am. Ceram. Soc.,* **83**, 353 – 361, (2000).

19 Lucato, S., Lupascu, D., Rödel, J.: Effect of poling direction on R-curve behavior in lead zirconate titanate, *J. Am. Ceram. Soc.,* **83**, 424 – 426, (2000).

20 Fett, T., Munz, D., Thun, G.: Bending strength of a PZT ceramic under electric fields, *J. Eur. Ceram. Soc.,* **23**, 195 – 202, (2003).

21 Lupascu, D.C., Aulbach, E., Rodel, J.: Mixed electromechanical fatigue in lead zirconate titanate, *J. Appl. Phys.,* **93**, 5551 – 5556, (2003).

22 Lupascu, D.C., Genenko, Y.A., Balke, N.: Aging in ferroelectrics, *J. Am. Ceram. Soc.,* **89**, 224 – 229, (2006).

23 Griffith, A.A.: The phenomenon of rupture and flow in solids, *Phil. Trans. Roy. Soc. London,* **A221**, 163 – 198, (1920).

24 Murakami, Y.: The stress intensity factor handbook. New York: Pergamon press. (1986).

25 Tada, H., Paris, P., Irwin, G.R.: The stress analysis handbook. St. Louis: Del research corporation, (1985).

26 Newman, J.C., Raju, I.S.: An empirical stress-intensity factor equation for the surface crack, *Eng. Fract. Mech.,* **15**, 185 – 192, (1981).

27 Morrell, R.: Fractography of brittle materials, vol. 15. Teddington: National physical laboratory, (1999).

28 Jayatilaka, A., Trustrum, K.: Statistical approach to brittle fracture, *J. Mater. Sci.,* **12**, 1426 – 1430, (1977).

29 Danzer, R., Lube, T., Supancic, P., Damani, R.: Fracture of advanced ceramics, *Adv. Eng. Mat.,* **10**, 275 – 298, (2008).

30 Weibull, W.: A statistical theory of the strength of materials, pp. 45 Vol. 151. Stockholm: Generalstabens litografiska anstalts förlag. (1939).

31 Weibull, W.: A statistical distribution function of wide applicability, *J. Appl. Mech.,* **18**, 293 – 298, (1951).

32 Danzer, R.: A general strength distribution function for brittle materials, *J. Eur. Ceram. Soc.,* **10**, 461 – 472, (1992).

33 Bermejo, R., Sestakova, L., Grünbichler, H., Lube, T., Supancic, P., Danzer, R.: Fracture mechanisms of structural and functional multilayer ceramic structures, *Key Eng. Mat.,* **465**, 41 – 46, (2011).

34 Oates, W.S., Lynch, C.S., Lupascu, D.C., Kounga Njiwa, A.B., Aulbach, E., Rödel, J.: Subcritical crack growth in lead zirconate titanate, *J. Am. Ceram. Soc.,* **87**, 1362 – 1364, (2004).

35 EN 843 – 1, Advanced Technical Ceramics, Monolithic Ceramics, Mechanical Properties at Room Temperature, Part 1: Determination of flexural strength. EN, (1995).

36 ISO 23146, Fine Ceramics (Advanced Ceramics, Advanced Technical Ceramics) – Test Methods for Fracture Toughness of Monolithic Ceramics – Single-Edge V-Notch Beam (SEVNB) Method. ISO, Switzerland, (2008).

37 Anstis, G.R., Chantikul, P., Lawn, B.R.: A critical evaluation of indentation techniques for measuring fracture Toughness: I, direct crack measurements, *J. Am. Ceram. Soc.,* **64**, 533 – 538, (1981).

38 Bermejo, R., Gruenbichler, H., Kreith, J., Auer, C.: Fracture resistance of a doped PZT ceramic for multilayer piezoelectric actuators: Effect of mechanical load and temperature, *J. Eur. Ceram. Soc.,* **30**, 705 – 712, (2010).

39 Fett, T., Munz, D., Thun, G.: Nonsymmetric deformation behavior of lead zirconate titanate determined in bending tests, *J. Am. Ceram. Soc.,* **81**, 269 – 272, (1998).

40 Bermejo, R., Deluca, M.: Layered ceramics. In: Handbook of Advanced Ceramics, 2nd edition. Edited by S. Somiya and M. Kaneno, Tokyo, (2012).

41 Bermejo, R., Danzer, R.: Failure resistance optimisation in layered ceramics designed with strong interfaces, *J. Ceram. Sci. Tech.,* **01**, 15 – 20, (2010).

42 Bermejo, R., Torres, Y., Baudin, C., Sánchez-Herencia, A.J., Pascual, J., Anglada, M., Llanes, L.: Threshold strength evaluation on an Al_2O_3-ZrO_2 multilayered system, *J. Eur. Ceram. Soc.,* **27**, 1443 – 1448, (2007).

[43] Mizoguchi, K., Nakashima, S.-I.: Determination of crystallographic orientations in silicon films by raman-microprobe polarization measurements, *J. Appl. Phys.,* **65**, 2583 – 2590, (1989).

[44] Deluca, M., Higashino, M., Pezzotti, G.: Raman tensor elements for tetragonal BaTiO and their use for in-plane domain texture assessments, *Appl. Phys. Lett.,* **91**, 091906, (2007).

[45] Deluca, M., Sakashita, T., Galassi, C., Pezzotti, G.: Investigation of local orientation and stress analysis of PZT-based materials using micro-probe polarized raman spectroscopy, *J. Eur. Ceram. Soc.,* **26**, 2337 – 2344, (2006).

[46] Deluca, M., Bermejo, R., Gruenbichler, H., Presser, V., Danzer , R., Nickel, K. G.: Raman spectroscopy for the investigation of indentation-induced domain texturing in lead zirconate titanate piezoceramics, *Scripta Mater.,* **63**, 343 – 346, (2010).